Dynamics of the Four-Atom BO + H_2 → HBO + H Reaction: Potential Energy Surface and Reaction Selectivity from QCT Calculations

J. Sogas, M. Albertí, X. Giménez, R. Sayós, and A. Aguilar*

Departament de Química Física, Universitat de Barcelona, Martí i Franquès, 1, 08028 Barcelona, Spain

Received: May 8, 1997; In Final Form: September 5, 1997[⊗]

A six-dimensional potential energy surface (PES) for the adiabatic ground electronic state has been developed and quasiclassical trajectory calculations (QCT), focusing on selectivity of vibrational and rotational initial states upon reactive cross sections, have been performed for the title reaction BO + H_2 → HBO + H. It constitutes the first dynamical study of this four-atom reaction, for which the specified reaction channel is the only one open at moderate energies, the HOB + H channel being open at an energy of 55 kcal/mol above reactants. An analytical PES has been developed based on a Sorbie−Murrell many-body expansion, giving rise to a monovalued, smooth function which correctly reproduces the most important features of the interaction potential. Extended QCT calculations have been performed for low and moderate collision energies, which have led to a proper characterization of the excitation function shape. Additional extended calculations covered several vibrational and rotational initial states, so that selectivity upon reactivity has been studied in detail. Noteworthy features are the clear enhancement of the reactive cross section as the H_2 vibration is increased and the inhibition of the reactivity as the BO vibrational energy is higher, which have been interpreted in terms of the characteristics of the transition state normal mode(s) correlating with the corresponding asymptotic states. It has been also found that several dynamical features are easily explained as a consequence of the collinearity of the transition state.

I. Introduction

In recent years, relevant improvements in both experimental and theoretical methodologies have led to an increased amount of information concerning the dynamics and kinetics of gas-phase elementary four-atom reactions.[1−7]

Development in experimental techniques have permitted the appearance of detailed state-selected and state-to-state reaction dynamics and kinetics studies, involving both neutral and ionic species,[3−7] which have led to a noticeable increase in the understanding of several basic aspects related to four-atom elementary chemical reactions. Thus, for instance, the study of the influence of the additional vibrational modes not present in atom−diatom systems has evidenced unusual enhancements and inhibitions of the reactive cross section. This latter feature can be expected to have important consequences as far as the selective control of chemical reactions is concerned.[4]

From the theoretical side, continuous improvements in both methodological and computational capabilities made it possible, during the past years, to extend the size and complexity of the systems being treated. Methods used were first quasiclassical and more recently quantum mechanical, the development of the latter having concentrated on a greater methodological effort. Thus, for instance, the availability of new or improved differential equation numerical integrators,[8,9] the use of better adapted coordinate systems,[10] and new techniques for solving the eigenvalue and eigenvector problem,[11] as well as the availability of the massively parallel and gigabyte core memory computers,[12] allowed the appearance of an important number of theoretical works on rather involved three-atom systems and, more recently, rather accurate studies on simple four-atom systems.

The comparison between the above detailed experimental results and the already essentially exact theoretical dynamical predictions—at least for a few benchmark systems[13−15]—is very strongly dependent on the availability, first, and reliability, second, of the potential energy surface (PES) associated to the reaction process. This fact constitutes an important bottleneck for the field. Some progress has been made in obtaining information about the PES from experimental measurements.[16] However, as far as reactive processes are concerned, it is still scarce, since it does not provide sufficient accurate information so as to properly describe the whole relevant region of configuration space. Ab initio quantum chemistry has been very often an excellent alternative for providing information on those missing regions, but the difficulties in computing the correlation energy, for the usually loose configurations near the transition state region, make necessary scaling procedures to match with the experimental data, thus introducing an undesirable empiricism to the process. Finally, the subsequent fit to an always complicated functional form (direct dynamics methods still prove to be extremely expensive for accurate computations[17]) is an involved task with an important component of ad hoc modifications and refinements. The situation is especially critical in four-atom reactions, for which very few reliable potential energy surfaces exist and then efforts to produce these functions for new systems are necessary.

Our group has been involved, during past 15 years, in the theoretical study of several three-atom reactions and, more recently, initiated in the field of four-atom elementary reactions with the study of the B(^{2}P) + H_2O,[18] the O(^{3}P) + CS_2,[19] and the O(^{1}D) + N_2O[20] reactions. For these reactions, potential energy surfaces and QCT calculations were performed, aimed at characterizing their reaction dynamics.

Of special interest, relevant to the present work, has been the study of the boron−water family of reactions. The boron oxidation process, which is very exothermic and provides considerably more chemical energy per unit volume of fuel than do conventional hydrocarbon-based fuels, has been then considered as a good candidate for being a rocket fuel.[21] However,

* To whom correspondence should be addressed.

[⊗] Abstract published in *Advance ACS Abstracts,* October 15, 1997.

S1089-5639(97)01561-2 CCC: $14.00

it presents some difficulties when practical implementation is considered. On the one hand, an intermediate solid-state boron oxide is formed which induces passivation over metallic boron. On the other hand, and more related to the kind of studies we are dealing with, the metastable HBO, HOBO, and HOBH oxyhydrides can be formed in the way to the complete oxidation to B_2O_3, thus diminishing the global energetic performance of the process. In addition to that, the knowledge of the complete mechanism is made difficult by the lack of kinetics information on the elementary steps involving the formation of the above metastable species.

The above reasons motivated a previous characterization of the multiarrangement channel B + H_2O reaction, for which a PES was developed and QCT calculations were performed.[18] The main result was that the HOB + H product was the dominant among the four possible ones. However, at the typical temperatures of the boron combustion, the exothermic BO + $H_2 \rightarrow$ HBO + H reaction is expected to have an important role in the complete reaction mechanism. For instance, it is one of the possible sources of the metastable species HBO. In addition, HOBH has been identified in the PES describing the above reaction. It appears then clear enough that the title reaction deserves a detailed reaction-dynamics study.

In addition to its practical interest, the title reaction is a fairly simple process for which the only possible rearrangement channel, at moderate energies, is the HBO + H, the HOB + H channel being reachable only above 55.7 kcal/mol. On the other hand, the HBOH system has relatively few electrons, thus being a good candidate for high-quality ab initio quantum chemistry calculations, so that future refinements of the PES are clearly expectable (once available, for instance, detailed experimental studies). Furthermore, this system is isoelectronic to the widely studied CN + H_2 system, with the BO mass being also very similar to the CN mass. For all these reasons, it is a system for which it is claimed to have also a fundamental interest, since it can be a candidate for benchmark calculations and testing of the general dynamical trends currently under development in the four-atom field. A main drawback, from the experimental point of view, is the relatively small cross section characterizing the reactivity of the system, which may result in an important difficulty for detailed, state-specific or state-to-state molecular beam experiments in order to obtain accurate data.[22]

Little work is available on this reaction from the literature. From the experimental side, rate constants have been measured between 690 and 1030 K by means of a pump-and-probe technique on a high-temperature reactor, and results were subsequently compared to transition-state-theory calculations. The authors report values lying between $(0.97 \pm 0.15) \times 10^{-13}$ cm^3 s^{-1} at 689 ± 40 K and $(9.0 \pm 1.3) \times 10^{-13}$ cm^3 s^{-1} at 1029 ± 86 K.[23] A previous theoretical work is available, in which the reactants, transition state and products were studied using ab initio MCSCF and multireference CI techniques, with a basis set up to triple-ζ plus double polarization quality. The exothermicity and reaction barrier were calculated, obtaining values of 6.4 and 9.5 kcal/mol, respectively. A main result of this work was the recomendation of a new and considerably more negative value of the standard heat of formation of HBO, −60 kcal/mol.[21]

The present work is mainly intended at characterizing, for the first time, the detailed dynamics of the BO + $H_2 \rightarrow$ HBO + H reaction. To this end, the first stage consisted in developing an accurate, but as simple as possible, six-dimensional potential energy surface. Then, the second stage of the work was based on a detailed QCT study, aimed at characterizing the reaction dynamics of the system, with special emphasis on the selectivity of each initial state upon reactivity. The paper is organized as follows: section II describes the details of the PES here developed. In section III the main results corresponding to the QCT calculations are presented and subsequently analyzed in section IV. Finally, the most important conlusions are summarized in section V.

TABLE 1: Parameters for the Two-Body Terms of the PES Function

	a/Å^{-1}	D_e/eV	R_e/Å
BO($^2\Sigma^+$)	3.6800	7.7486	1.1870
BH($^3\Pi$)	3.3508	2.3939	1.1795
OH($^3\Pi$)	3.7197	4.1470	0.9547
H_2($^1\Sigma_g^+$)	2.9624	4.5357	0.7326

II. Potential Energy Surface

The analytical potential energy surface for the title reaction was obtained using the same Sorbie−Murrell method that was successfully applied to B + H_2O,[18] O + CS_2,[19] and other reactions.[24] The basis of the method consists in assuming that the overall interaction potential for a four-body system can be expressed as a sum of mono-, bi-, tri-, and tetraatomic terms, in the form

$$V_{ABCD} = \sum_A V_A^{(1)} + \sum_{AB} V_{AB}^{(2)}(R_{AB}) + \sum_{ABC} V_{ABC}^{(3)}(R_{AB},R_{BC},R_{CA}) + V_{ABCD}^{(4)}(R_{AB},R_{AC},R_{AD},R_{BC},R_{BD},R_{CD}) \quad (1)$$

Since reactants and products of title reaction correlate in their ground electronic states, all atoms have been considered in their ground electronic states and the monatomic terms have been taken to be zero, as is usual. Diatomic terms are expressed by means of Rydberg functions:

$$V_{AB}^{(2)}(\rho) = -D_e(1 + a\rho)e^{-a\rho} \quad (2)$$

where

$$\rho = R_{AB} - R_{AB,eq} \quad (3)$$

D_e being the dissociation energy and $R_{AB,eq}$ the equilibrium internuclear distance. The a coefficient is related to the diatomic harmonic force constant. The three parameters of all the diatomic fragments were determined by the best fit to theoretical calculations.[25−28] Table 1 shows the optimal adjusted parameters determined for the BO, BH, OH, and H_2 fragments.

Among the six possible triatomic fragments, HBO, H′BO, HOB, H′OB, H_2O, and BH_2, the last two have not been included in the PES since they lie well above the energies of the present study. In particular, they lie 3.5314 (H_2O) and 5.4631 (BH_2) eV above the BO + H_2 assymptotic channel, and the present study has been limited to the 0−1.5 eV energy range. Each one of the triatomic terms has been chosen to be of the type

$$V_{ABC}^{(3)} = P(\rho_{AB},\rho_{BC},\rho_{CA})\cdot T(\rho_{AB},\rho_{BC},\rho_{CA}) \quad (4)$$

with

$$P(\rho_{AB},\rho_{BC},\rho_{CA}) = V_0\{1 + \sum_i c_i\rho_i + \sum_{ij} c_{ij}\rho_i\rho_j + \sum_{ijk} c_{ijk}\rho_i\rho_j\rho_k\} \quad (5)$$

$$T(\rho_{AB},\rho_{BC},\rho_{CA}) = \prod_i \left\{1 - \tanh\left(\frac{\gamma_i\rho_i}{2}\right)\right\} \quad (6)$$

and being i, j, k = AB, BC, or CA. The displacement

TABLE 2: Parameters for the Three-Body Fragment HBO (R1, R2, R4) of the PES[a]

V_0	−2.3888 eV				
c_1	0.0640 Å^{-1}	c_{22}	0.2661 Å^{-2}	γ_1	3.925 Å^{-1}
c_2	−1.7893 Å^{-1}	c_{24}	−2.2514 Å^{-2}	γ_2	0.425 Å^{-1}
c_4	3.2157 Å^{-1}	c_{44}	3.4489 Å^{-2}	γ_4	2.400 Å^{-1}
c_{11}	0.4440 Å^{-2}	c_{124}	−16.1359 Å^{-3}	R_1°	1.18542 Å
c_{12}	−2.6342 Å^{-2}	c_{222}	−4.3204 Å^{-3}	R_2°	1.16485 Å
c_{14}	3.5274 Å^{-2}	c_{444}	2.0899 Å^{-3}	R_4°	2.35027 Å

[a] Numerical indexes correspond to 1 ≡ BO; 2 ≡ BH; 4 = OH. The same results as for HBO (R1, R2, R4) are valid for the HBO (R1, R3, R5) potential function, changing 2 to 3 and 4 to 5.

coordinates are defined, in the case of the triatomic fragments, as

$$\rho_{BO} = R_{BO} - R_{BO}^\circ \tag{7}$$

$$\rho_{BH} = R_{BH} - R_{BH}^\circ$$

$$\rho_{OH} = R_{OH} - R_{OH}^\circ$$

with R_i° corresponding to the distances defining a reference structure. In the present case, it was convenient to choose it to be the geometry corresponding to the stable species HBO, whose geometry has been determined by means of high-level ab initio calculations.[28] Table 2 shows the parameters characterizing the HBO, H′BO, HOB, and H′OB triatomic fragments. The optimal parameters have been obtained by fitting the dissociation energies, the geometry, and the force constants of the triatomic species.[25−28]

The necessity of a four-body term to properly describe the potential energy surface can be evidenced as follows. From previous ab initio calculations,[21] it has been determined that the reaction pathway is collinearly dominated and has an energy barrier of 9.5 kcal/mol, this findings being consistent with the experimental data.[23] If the PES is represented, within the collinear restriction, with a function including up to the three-body term (Figure 1), it is found a minimum instead of a maximum in the strong interaction region. Thus, a four-body term needs to be included to correct this fact. No general prescriptions exist to stablish the best function for the four-body term, so several cases, previously proposed in the literature,[24] were implemented. The best description of the overall features of the PES was obtained with a double four-body term of the form[29,30]

$$V_{HH'BO}^{(4)} = V_1^{(4)} + V_2^{(4)} \tag{8}$$

being each term:

$$V_j^{(4)} = V_{0j} \prod_i e^{-\gamma_{ij}\rho^2_{ij}} \tag{9}$$

with $j = 1, 2$; i = BO, BH, BH′, OH, OH′, HH′; $\rho_{ij} = R_i - R_{ij}^\circ$, corresponding the reference structure to the symmetric geometry given in Table 3, in which the best coefficients characterizing the tetratomic term are included along. In order to keep effort of the whole fitting process reasonable, these coefficients have been optimized to simply reproduce, as close as possible, the barrier height and the transition state geometry previously available from ab initio calculations.[21] It is interesting to note that the V_{0j} coefficients for each four-body term have opposite sign. This prevents the appearance of spurious minima and gives rise to proper values for the barrier height, thus facilitating the fitting procedure.

Potential energy contours of the global surface in the collinear restriction approach are shown in Figure 2. The transition state

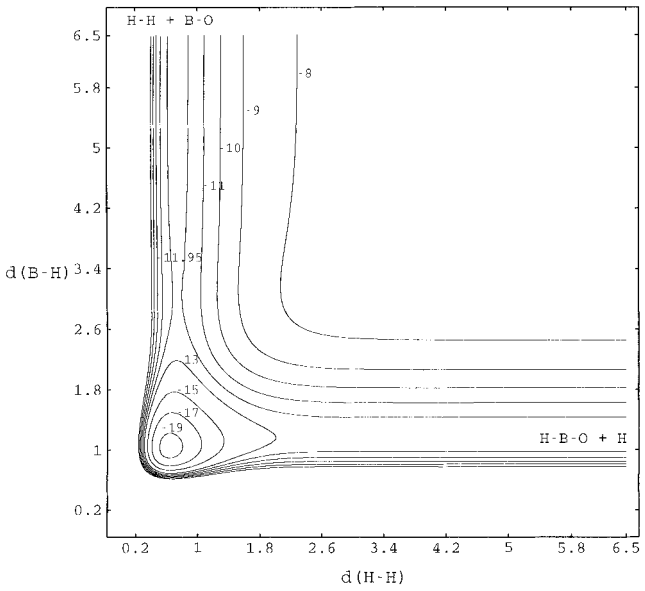

Figure 1. Potential energy contours (in eV), without the four-body term, in the collinear restriction and keeping fixed d(B−O) = 1.1825 Å (distances are in Å and zero energy is taken at separated atoms).

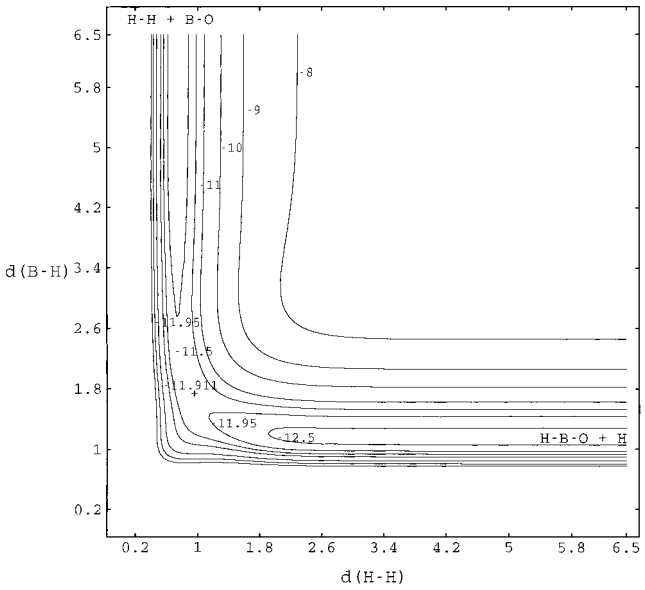

Figure 2. Potential energy contours (in eV) of the global surface within the collinear restriction and keeping fixed d(B−O) = 1.1825 Å (distances are in Å and the zero energy is taken at separated atoms).

configuration (located 8.62 kcal/mol above reactants) is also indicated in the plot, obtaining, as expected, a collinear geometry. Table 4 shows the numerical values for the distances corresponding to this transition state (TS) geometry. The contour plots have been obtained keeping fixed the BO distance to that corresponding to the transition state configuration. This is a rather correct representation, since it has been found that the BO distance, which describes the spectator bond, varies little in going from reactants to products.

A comprehensive research of critical points was undertaken, which led to the localization and characterization of the H_2BO (M1) and HBOH (M2) minima. These stable structures have been reported previously as a result of some ab initio calculations,[25−28,31] but not quoted in other works.[21] The first minimum has C_{2v} symmetry and only its geometry is well reproduced in the present surface. However, as will be explained below, it has been found to have no direct influence on the reaction dynamics, so that its accurate description is not critical. The second minimum shows a trans geometry and both

TABLE 3: Parameters for the Four-Body Term of the PES[a]

j	1	2
V_{0j}/eV	17.20	−8.47
R°_{1j} /Å	1.201	1.200
R°_{2j} /Å	1.193	1.955
R°_{3j} /Å	1.193	1.955
R°_{4j} /Å	2.041	2.020
R°_{5j} /Å	2.041	2.020
R°_{6} /Å	0.715	1.061
γ_{1j}/Å^{-2}	−19.550	−5.000
γ_{2j}/Å^{-2}	0.373	0.1138
γ_{3j}/Å^{-2}	0.373	0.1138
γ_{4j}/Å^{-2}	0.191	0.630
γ_{5j}/Å^{-2}	0.191	0.630
γ_{6j}/Å^{-2}	0.565	1.000

[a] Numerical indexes correspond to: 1 ≡ BO; 2 ≡ BH; 3 ≡ BH′; 4 ≡ OH; 5 ≡ OH′; 6 ≡ HH′.

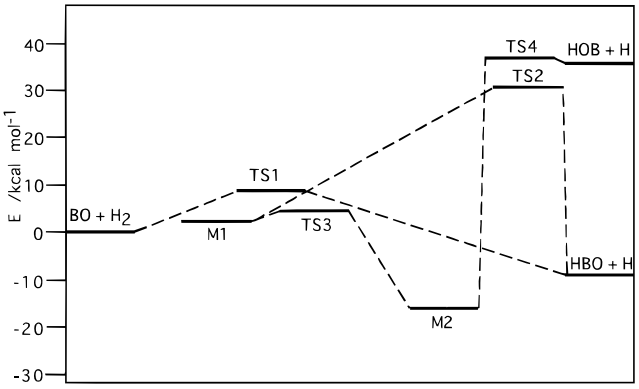

Figure 3. Schematic energy profile on the analytical PES, referred to the reactants' energy.

TABLE 4: Geometry of the Reaction Transition State as Obtained in the Analytical PES

R_{BO}/Å	R_{BH}/Å	R_{HH}/Å	O−B−H/°	B−H−H′/°
1.1825	1.6893	2.6299	180.0	180.0

geometry and energetics have been well reproduced. Figure 3 shows a scheme of the critical points and pathways interconnecting them as found in the comprehensive exploration of the global PES. As a result, three additional transition states have been identified. Due to symmetry considerations, no direct reaction path has been found connecting the minima with the reactants asymptote, as previously found in the literature.[31] The above minima are only involved with the alternative reaction path leading to HOB + H, which is reachable through a transition state located 55.7 kcal/mol above the M2 minimum. Thus, it is expected to have a small influence, at low and moderate energies, in the reaction mechanism.

III. Results of the Quasiclassical Trajectory Calculations

QCT calculations for the BO + H_2 reaction, on the above global PES, were performed by means of the POLQCT program[32] which was developed in our group. Numerical integration of Hamilton equations was made through a fourth-order Runge−Kutta−Gill method combined to a sixth-order predictor−corrector Adams−Moulton algorithm with fixed step size. Reactive trajectories have been classified according to an indexation by which the channels BO + H_2, H′BO + H, HBO + H′, H′OB + H, and HOB + H′ correspond to I, II, III, IV, and V, respectively. Channels II and III are completely equivalent, being the same for IV and V. The rest of the possible rearrangement channels have not been included due to energetic considerations.

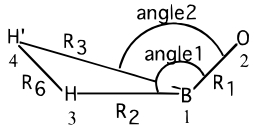

Figure 4. Reference structure used for identification of distances, angles, and dihedrals represented in the trajectory plots.

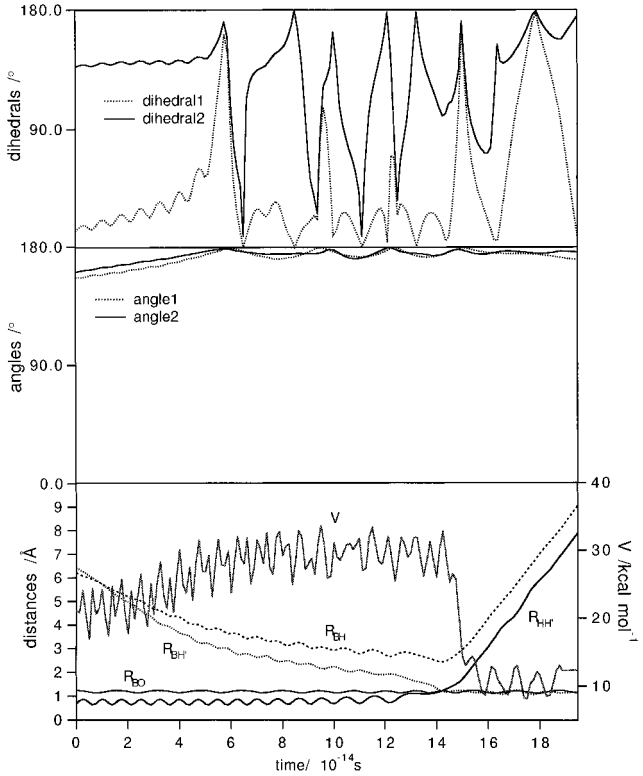

Figure 5. Time evolution of the geometrical parameters and potential energy for a reactive trajectory leading to HBO + H. E_{trans} = 9 kcal mol^{-1}; reactants' vibrotational level: BO(0,7), H_2(0,1). The zero energy is set to the lowest minimum, M2.

The main numerical features characterizing the calculations are the following. The time step size has been fixed to 1.25 × 10^{-16} s, being enough to accomplish an energy and momentum conservation lower than 0.01%. The quasiclassical trajectory initial conditions fixed in each calculation have been the vibrotational quantum numbers (v,J) of both reactant diatomic molecules, the relative translational energies (E_{trans}), the maximum impact parameter (b_{max}), and the initial distance between the centers of mass of the reactant molecules (ρ_0). The remainder of the necessary initial conditions, i.e., the orientation between molecules and the impact parameter (b), have been selected randomly following the Monte Carlo Method,[33] as usual.

Reaction Mechanism. Individual inspection of each reactive trajectory gives valuable information about the general trends governing the reaction mechanism. Figures 5−7 show representative trajectories covering relevant initial conditions. In these figures the distances and angles represented are indicated: dihedrals 1 and 2 are defined respectively by the planes 213 and 431, and 231 and 432 (see Figure 4). A first remarkable important point is the direct abstraction mechanism found for all reactive trajectories. No complex trajectories have been detected, so that neither the M1 nor the M2 minima are probed in the reaction pathway. This can be additionally confirmed by plotting the potential attained at each point of the trajectory. It is found that no configurations whose potential energy lies below the products assymptote are reached. On the another hand, the maximum potential energy essentially corresponds,

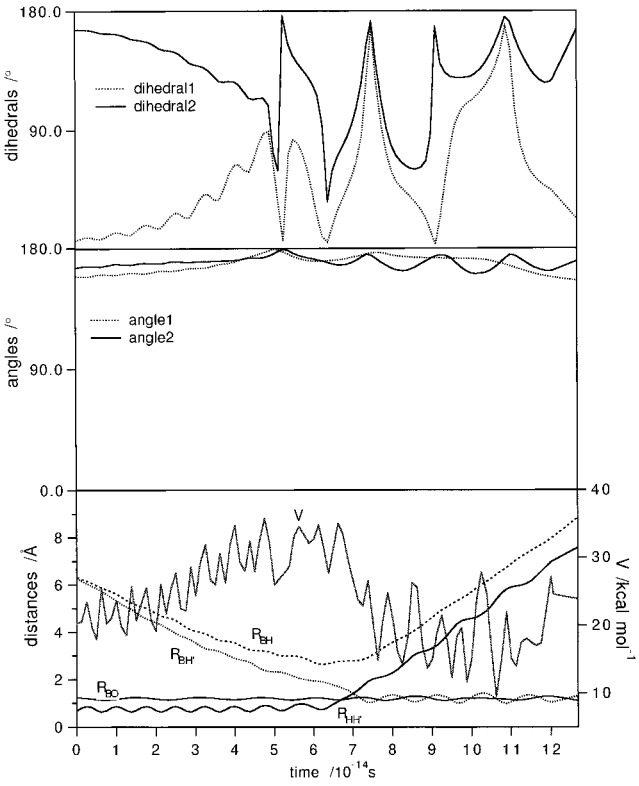

Figure 6. Same as Figure 4. E_{trans} = 18 kcal mol^{-1}.

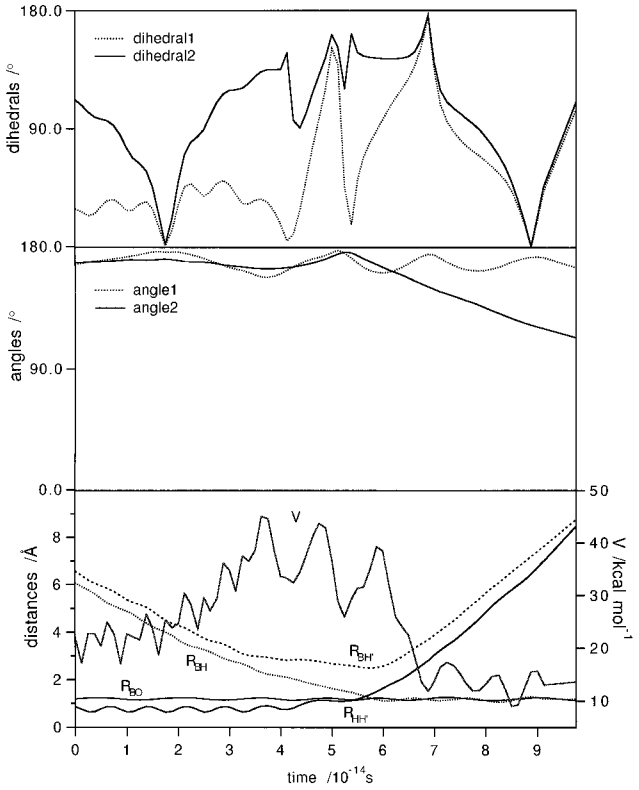

Figure 7. Same as Figure 4. E_{trans} = 35 kcal mol^{-1}.

once averaged over vibrations, to the transition state configuration region. Thus, it is possible to neglect the influence on the collision of either the M1 and M2 minima or the hypothetical path connecting M1 with reactants. In addition, no trajectories ending in the HOB + H′ (or H′OB + H) channel have been found. This makes the poorer description of the M1 energetics, as compared to M2, less relevant in the present study.

Another important point to be stressed here is the strong tendency to collinearity of each individual collision. In particular, both represented angles, in Figures 5−7, take values very close to 180° when all atoms are closest. Additional interesting features are the almost invariance of the BO stretch motion during the collision, in accordance with the essentially spectator role of the nonreactive bond in four-atom collisions, as established in several previous works concerning, for instance, H_2 + OH[13−15,34−38] and H_2 + CN.[39−41] However, it will be found to have a nonnegligible effect when a higher amount of vibration is put into this nonreactive bond.

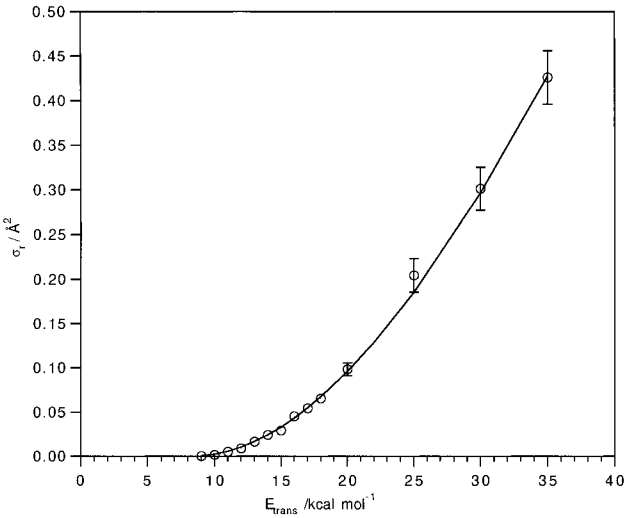

Figure 8. Total reactive cross sections vs translational energy. Reactants' vibrotational level: BO(0,7), H_2(0,1). Errors (one standard deviation) for lower energies are omitted due to their small values. The solid line shows the best fitting using an ADLOC function.

Reactive Cross Sections. The excitation function has been determined for several collision energy values according to the standard expression and with a standard deviation given by the usual formula.[33]

Integral cross sections have been obtained in the 9−35 kcal/mol energy range, for a total of 15 energy values, requiring up to 2 500 000 trajectories in order to get correct statistics. This large number was due to the rather small reactivity obtained, mainly in the low-energy regime.

Figure 8 shows the integral cross section as a function of collision energy, for reactants in the $v = 0$, $J = 7$ (BO) and $v = 0$, $J = 1$ (H_2) energy levels, which are the most populated at 300 K. It displays the typical shape of reactions having a barrier, with the particular feature of showing a continuous increase with no saturation. This fact is attributable to high-frequency vibrational motions perpendicular to the reaction path, which makes the corresponding potential profiles to be highly repulsive. As a consequence, saturation is only reachable at very high energies, since for low and moderate ones there is a continuous but slow increase of the reactive flux as the multidimensional generalization of the window-to-reaction concept, often used in triatomic reactions,[42−45] gets slowly wider.

Effect of Rotational and Vibrational Excitation on Reactivity. Figures 9 and 10 show the influence of rotation. This study has been performed at a collision energy of 18 kcal/mol, with reactants in their ground vibrational levels. In Figure 9, the rotational energy of H_2 was kept and the rotation of BO was varied, and vice versa for Figure 10. The effect in both cases is very similar, resulting in a reactivity decrease as the rotational energy is increased. However, two general cases can be distinguished, depending on whether the rotational energy of the "fixed" molecule was kept as zero or not. As a propensity rule, we can state that if rotational energy is zero, a continuous decreasing shape is obtained, while a maximum appears for higher rotational energies.

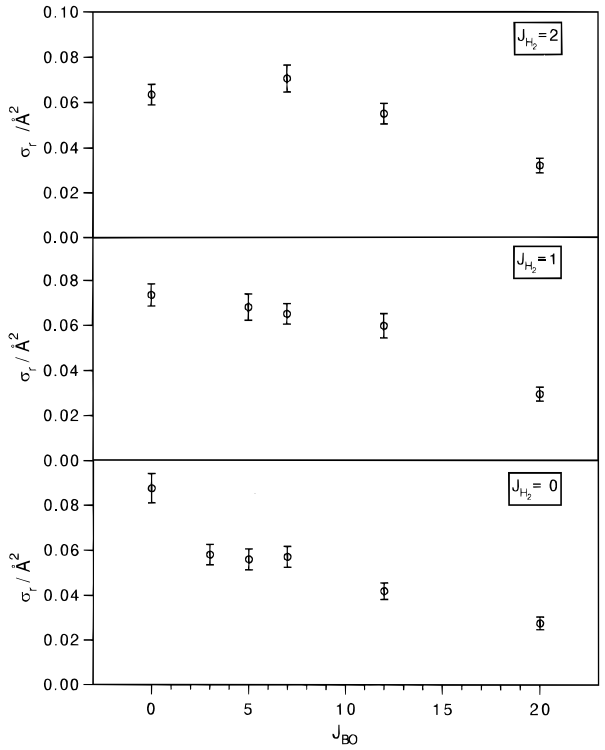

Figure 9. Reaction cross section as a function of J_{BO} at different J_{H_2} values. $E_{trans} = 18$ kcal mol^{-1} and $v_{BO} = v_{H_2} = O$.

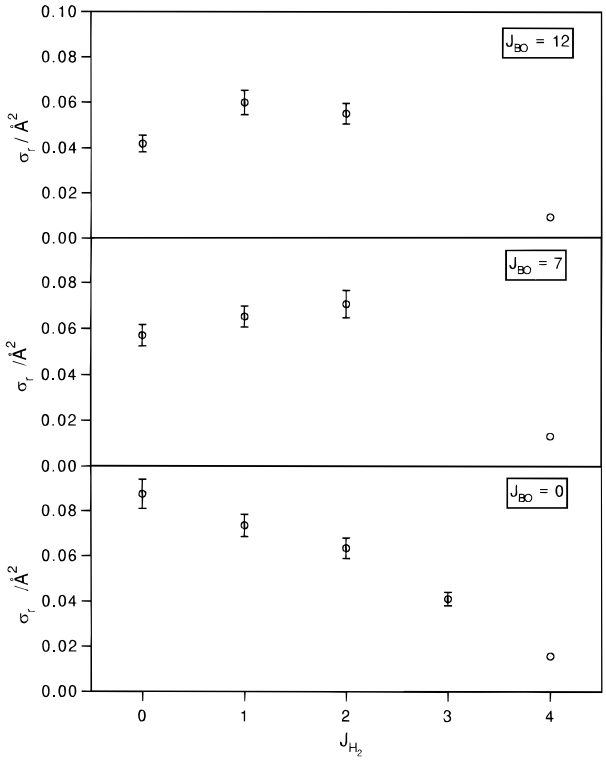

Figure 10. Reaction cross section as a function of J_{H_2} at different J_{BO} values. $E_{trans} = 18$ kcal mol^{-1} and $v_{BO} = v_{H_2} = 0$.

The effect of vibration is studied in Figures 11 and 12, for several relative translational energies and for reactants in their ground rotational levels. Strictly speaking, what has been studied is the effect of vibration for different initial translational energies and the effect of translation for different initial vibrational levels, keeping always fixed the rotational energy of both reactant molecules. The effect of translation is clearly evidenced in Figure 11. For each given initial vibrational level, an increase in translational energy monotonously increases the

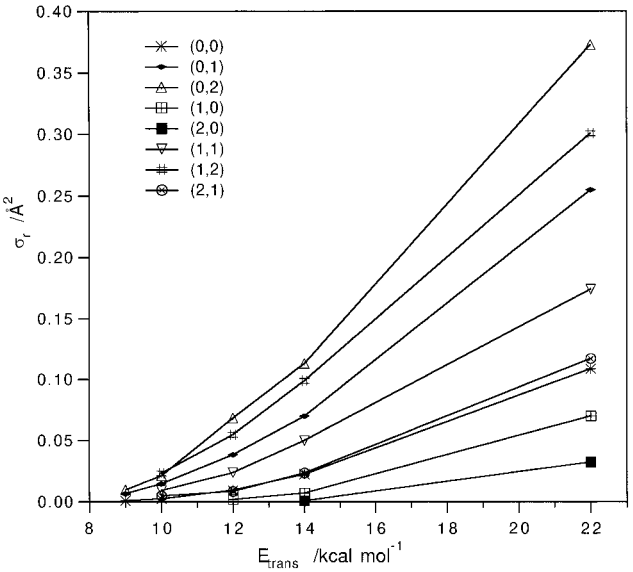

Figure 11. Total cross section vs translational energy at different reactants vibrotational levels for the reactants. Numbers in parentheses are (v_{BO}, v_{H_2}). $J_{BO} = J_{H_2} = 0$.

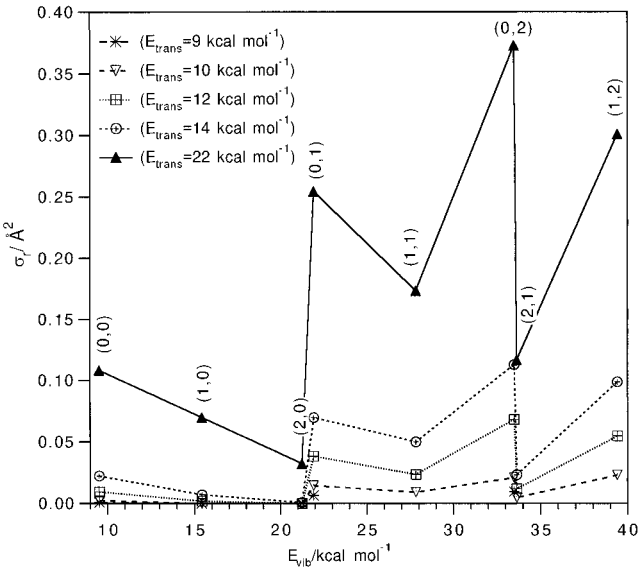

Figure 12. Reaction cross section as a function of vibrational energy. Numbers in parentheses are (v_{BO}, v_{H_2}). $J_{BO} = J_{H_2} = 0$.

reactivity, resulting in different curves (for each different vibration) which never cross. On the other hand, the effect of vibrational energy as a whole is shown in Figure 12. The *x* axis has been deliberately chosen to be an energy axis (rather than a vibrational level axis) to make explicit the fact that what is important is *where* the vibrational energy is put, i.e., the bond or normal mode being excited, and not the *amount* of vibrational energy. However, each vibrational energy considered has attached to it a label associated to the vibrational quantum numbers. In this way, it is possible to easily identify two initial states having almost the same vibrational energy which give rise to reactivities differing by near 1 order of magnitude, as occurs for the (2,0) and (0,1) case (being (v_1,v_2) the vibrational quantum numbers of the BO and H_2 molecules, respectively). A similar behavior is found for the (2,1) and (0,2) case.

On the other hand, it is found that translational energy is more effective than vibrational energy for promoting reactivity. This can be evidenced by comparing collisions with the same available energy but different internal energy distributions. Thus, for instance, the (0,1) case with $E_{trans} = 18$ kcal/mol (48.845

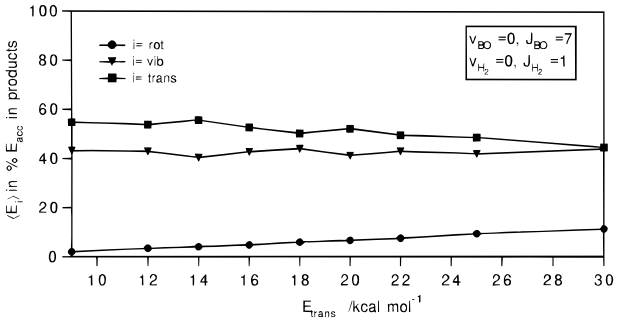

Figure 13. Energy distribution in products at different translational energies. $v_{BO} = v_{H_2} = 0$; $J_{BO} = 7$; $J_{H_2} = 1$.

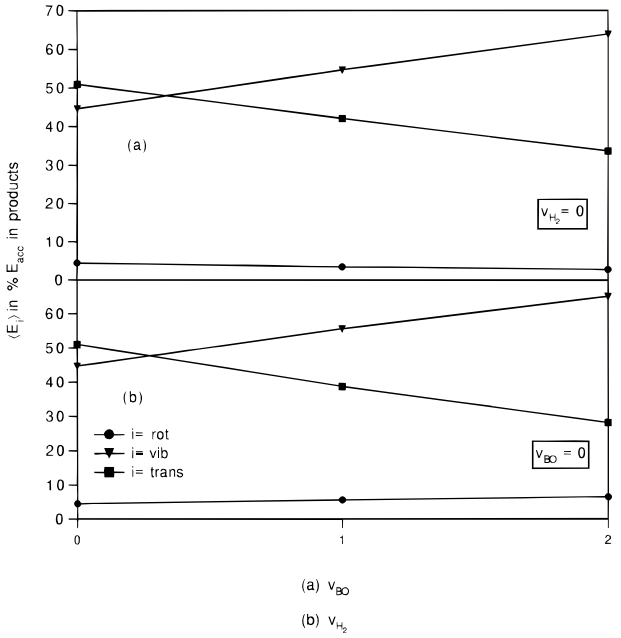

Figure 14. Energy distribution in products at different vibrational levels. $J_{BO} = J_{H_2} = 0$; $E_{trans} = 18$ kcal mol^{-1}. (a) $v_{H_2} = 0$; (b) $v_{BO} = 0$.

kcal/mol of available energy) has a cross section of 0.148 Å,^{2} while the same quantity for the (0,0) case with $E_{trans} = 30$ kcal/mol (48.434 kcal/mol of available energy) equals 0.284 Å.^{2}

As far as vibrational energy is concerned, a general propensity rule which appears to apply here is that an increase in H_2 vibration, i.e., the reactive bond, clearly enhances reactivity (as it can be evidenced following the (0,0), (0,1), and (0,2) labels), while an increase in BO vibration clearly inhibits reactivity, which can be seen, for instance, through the (0,0), (1,0), and (2,0) sequence. The above rule appears to be even more general, since it is found to be valid for levels having vibrational quanta in both reactant molecules as well as for all translational energies investigated. In addition, the qualitative pattern describing the cross section variation as a function of vibrational energy is the same independently of translational energy. This latter statement is an alternative way of evidencing the monotonic increase as translational energy is increased shown in Figure 11.

Product Energy Distribution. The energy partition among products has been studied in relation to the accessible energy (E_{acc}). It is shown, depending on the initial conditions, in Figures 13−16. As far as the dependence on translational energy is concerned, it can be seen that most (90%) of accessible energy is channeled into products translation (50%) and vibration (40%). An increase in translational energy only slightly modifies the relative distribution, increasing rotation

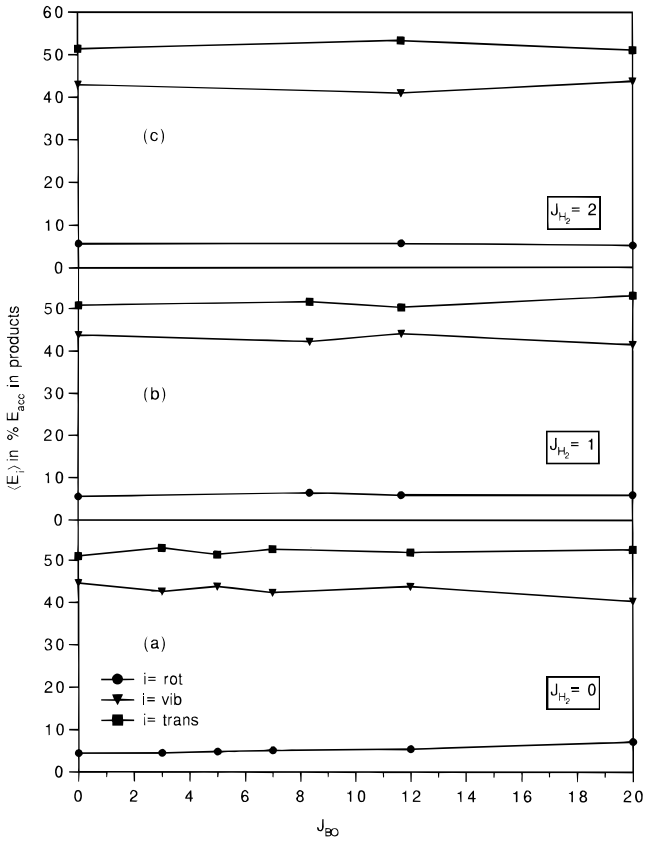

Figure 15. Energy distribution in products at different BO rotational levels. $v_{BO} = v_{H_2} = 0$; $E_{trans} = 18$ kcal mol^{-1}. (a) $J_{H_2} = 0$; (b) $J_{H_2} = 1$; (c) $J_{H_2} = 2$.

in the same amount that translation is decreased. Vibrational energy is nearly unaltered.

On the other hand, an increase in reactants, vibrational energy results in a clear increase of products vibrational energy as the main effect. Finally, the effect of rotational energy is very small, for which it is found an essentially constant trend as reactant's rotation is increased. It is interesting to point out here that the effects of both reactants vibrational and rotational energy are independent of where the energy is put; i.e., they are nearly insensitive to the bond that is being either vibrationally or rotationally excited.

IV. Discussion

The first comment will be addressed to the role of the spectator bond. Previous theoretical studies on the OH + H_2,[13−15,34−38] CN + H_2,[39−41] Cl + HOD[46] reactions, for instance, assign to the nonreactive bond a near to null influence on reactivity, for which it is stated that putting vibrational energy into this bond leave results basically unaffected. However, it has been also clearly said that this result is not expected to be a general trend in polyatomic reactions, since additional conditions must be accomplished.[1] For instance, the nature of the normal mode at the transition state determines the dissociation to products. Putting energy into those bonds which will directly participate in the reaction normal mode enhances reactivity, while putting energy in those bonds or modes nonparticipating has no influence on reactivity. However, these conclusions are necessarily approximate, since coupling between different normal modes is neglected and this is only possible for particular PES topographies. For instance, most recently,[41] the nonnegligible influence of the CN bond (on a newly developed PES) on the CN + H_2 dynamics has been explained in terms of coupling between CH and CN stretch vibrations.

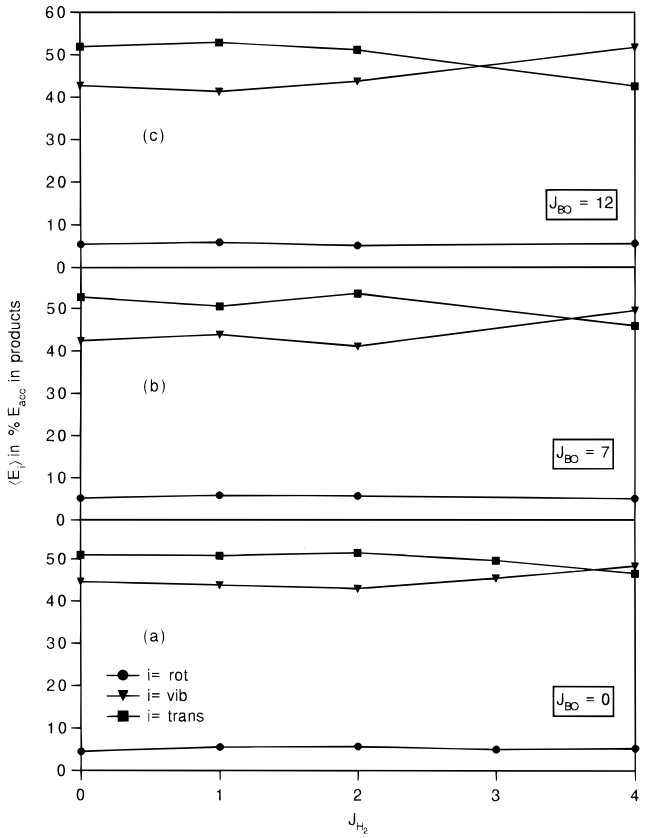

Figure 16. Energy distribution in products at different H_2 rotational levels. $v_{BO} = v_{H_2} = 0$; $E_{trans} = 18$ kcal mol^{-1}. (a) $J_{BO} = 0$; (b) $J_{BO} = 7$; (c) $J_{BO} = 12$.

For the BO + H_2 reaction, an inhibition rather than no influence is obtained when increasing the vibrational content of the BO molecule, while a clear reactivity increase is observed as the H_2 vibration is higher. This particular behavior is interpreted in the following terms. Figure 17 displays the set of normal modes, including the imaginary frequency normal mode, at the transition state. The TS modes which more purely correlate with the asymptotic H_2 vibration are ν_i and ν_3, since the remainder correspond to modes which tend to break up the collinearity and then must correlate with asymptotic states with a certain amount of either orbital or rotational angular momentum. The detailed inspection of both ν_i and ν_3 modes allows to see that ν_i tends to make the H−H distance bigger as the whole H_2 molecule approaches BO, being then the reactive mode, while ν_3 tends to shorten the H−H distance as H_2 gets closer to BO. Then, an increase in the H_2 vibrational content tends to both favoring the HBO + H formation, thus increasing reactivity, and the excitation of the ν_3 vibrational mode.

Due to equivalent correlation arguments, the BO asymptotic vibration essentially goes to the ν_4 mode, which is characterized by an increase of the B−O distance as BO approaches H_2. As the BO vibrational content is increased, the supermolecule then probes more and more the highly repulsive configurations of the O + BHH channel (for instance, the O + BH_2 channel is 5.4631 eV endoergic with respect to BO + H_2 or, equivalently, the ν_4 frequency is the highest one, being 3109.98 cm^{-1}). As a consequence, rebounding trajectories are expected to become more dominant as BO vibration is increased and thus induce a reactivity inhibition. These results are comparable to those recently obtained by Szichman and Baer,[47] who performed an approximate quantum-mechanical study of the NH + NO reaction. They show that when increasing the vibrational content of the NO molecule, reactivity is clearly inhibited (even in a higher amount than in our case), the reason being attributed

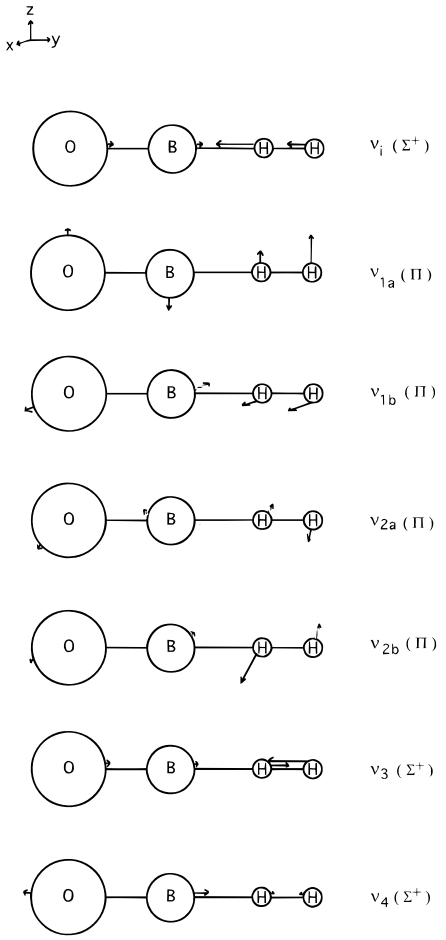

Figure 17. Schematic representation of the normal modes and the imaginary frequency normal mode at the transition state. The radius of spheres are proportional to the atomic masses.

to the fact that since the oxigen mass is very close to the nitrogen mass, the NH molecule is efficiently kicked back by the vibrating NO, thus complicating the exchange process. Comparison of both results with the previous calculations on OH + H_2,[13−15,34−38] CN + H_2,[39−41] Cl + HOD,[46] for which a milder to null inhibiting effect is obtained, seems to point out a proportionality between the mass of the spectator atom of the spectator bond and the amount of inhibition thus induced. However, this argument might be confirmed once more data on this feature will become available.

As for the differencies in the dynamical mechanism responsible for the vibrational inhibition, between Szichman and Baer's (SB) model and ours, it can be said that they seem to be complementary. If the collision is dominated by a sudden mechanism, the SB arguments are found to be sufficient to justify the observed behavior, gaining advantage from its higher simplicity. However, for low translational energy collisions or those dominated by vibrational adiabaticity, at least at the TS region, the normal-mode correlation analysis seem to be more adequate since collisions are slow enough to follow the normal-mode particularities of the TS region. In conclusion, in the latter case factors due directly to the PES topography may have to be added to the kinematic ones in order to explain the observed behavior.

An indicator of normal-mode separability, from the remainder of the coordinates describing the molecular motion, is the product energy partitioning variation as reactants vibrational energy is modified. Figures 13−16 clearly indicate that when either H_2 or BO vibrational content is increased, the amount of product vibrational energy is increased by nearly the same

quantity. This is a result that is expected for the case of BO, since its vibrational motion is found to be weakly coupled to the reaction coordinate, but, in principle, surprising for the H_2 case. It is possible to state then that a good representation of the reaction process is obtained assuming a vibrational sudden behavior, which results as a consequence of weak couplings between the different components of the molecular motion.

Several dynamical features emerge as a consequence of the strongly collinearly dominated PES. First, the rotational dependence of the cross section. The analysis of the rotational dependence of the reactivity is usually made in terms of the influence of orientation on the one hand and energetics on the other. By orientational effect it is usually meant that a change in rotational velocity means changing the availability of the proper configurations which lead to reaction, the result being either inhibiting reactivity for strongly oriented, repulsive surfaces or enhancing reactivity for nonoriented, attractive potentials. By the energetic effect we mean that concerned with the fact that a given amount of energy is trapped as rotation. Whether this effect will enhance or inhibit reactivity will depend on the kinematics and the topography of the PES, i.e., transition state geometry, degree of anysotropy, existence of strong interaction region complexes, etc. since these are the factors responsible for the necessary energy transfer between the rotational and reaction modes, if rotational energy must influence reactivity.

An increase in the rotational quantum number results in greater difficulties for allowing the system to collide with the proper, i.e., collinear, orientation. An indicator pointing toward this statement is the homogeneous decrease of the cross section as rotation is increased, being irrespective of the reactant molecule rotationally excited. Neither cross section corresponding to excited rotational states gives rise to a larger value than that corresponding to the ground rotational levels. This is the general trend. However, it is seen that a slight reactivity enhancement is found for intermediate rotational excitations of both reactant molecules (maxima in Figures 9c and 10b,c). This result can be interpreted as follows: the initial rotation of the target molecule causes disruption of the most favorable configuration (the collinear) in the TS zone. This effect can be partially compensated by slightly increasing the rotational energy of the attacking molecule, since then the collinear orientation is "pursued" thanks to the adequate rotational velocity of the attacking molecule. As the rotation of this attacking molecule is further increased, the proper orientations of both molecules do not match long enough and reactivity goes down.

The present results indicate that the orientational factor dominates over the energetic one or, in other terms, trapping energy as rotation does not enhance reactivity due to the lesser effectivity in orienting the system to the (rather) few favorable configurations.

The excitation function shape is due, as discussed in the previous chapter, to the strong collinearly dominated PES, as a consequence of the high frequency of some of the modes perpendicular to the reaction coordinate. This causes, on the one hand, the reactivity to be rather low, on the overall, since the density of states is quite small in the transition state region. In addition, as stated before from another point of view, its slow increase with energy causes that saturation of the cross section is never reached within the scanned energy range.

The QCT method has been very extensively probed to be a useful and powerful tool for describing many dynamical features characterizing elementary chemical reactions. However, using the QCT excitation function shape for calibrating the potential energy surface through comparison with experiments is a delicate task. For instance, the quasiclassical threshold reactivity results from the compensation of errors due to the neglection of tunneling, which pushes the QCT threshold to higher energies when compared with the experimental one, and the impossibility of considering the zero-point energy (ZPE), which tends to make the QCT threshold lower. These effects are specially important in polyatomic (concerning the ZPE), light-atom exchange (concerning tunneling) reactions like the present one. For these reasons, calculation of rate constants for polyatomic reactions having a barrier must lead to careful comparisons with experimental results.

QCT rate constants for the title reaction have been calculated, overall, to be 1 order of magnitude lower than experimental results, with the same error when compared with scaled transition-state-theory results.[23] In our opinion, improvement of the potential energy surface must emerge from a strong interaction between more detailed experiments, higher level ab initio calculations on critical points of the PES, and the application of both quasiclassical and quantum dynamical methods; otherwise, efforts may be meaningless. Work is in progress along this line, as far as the theoretical work is concerned in our laboratory.

V. Conclusions

A six-dimensional potential energy surface for the title reaction has been developed and tested. It describes three rearrangement channels, corresponding to reactants and two product channels, the latter being those open at the energies of the present work. The potential surface shows, as main features, a barrier of 8.6 kcal/mol leading to the HBO + H channel, which is exothermic by 6 kcal/mol. The strong interaction region shows the existence of two tetratomic minima, H_2BO and HBOH, which are directly connected, through a transition state placed at 55.7 kcal/mol, to the alternative HOB + H channel, being 48 kcal/mol above reactants. No direct connection between reactants and the minima has been found.

The reaction dynamics has been studied by means of quasiclassical trajectories. The reaction mechanism is found to be described by direct, strongly collinearly dominated collisions. As a consequence, the remainder of the dynamical features are ultimately depending on it. The rotational dependence of the cross section shows a diminishing trend as rotation is increased, since the favorable orientations are hardly found when the molecules are rotating. However, it is found that an intermediate rotational excitation of both reactant molecules allows for an increase of the time the proper orientations coincide, giving rise to a slight reactivity enhancement. Vibrational energy leads to opposite results depending on whether the energy is put in the BO (inhibition) or the H_2 (enhancement) bonds. This behavior is interpreted in terms of the TS normal modes more purely correlating with the reactants asymptotic vibrations. Thus, it is found that H_2 vibration goes to the imaginary frequency normal mode, allowing then for reactivity enhancement. On the contrary, a BO vibrational increase causes inhibition since it basically goes to a normal mode which probes, under excitation, the repulsive configurations of the strongly exothermic O + BHH channel. This model for interpreting the role of the spectator bond has been compared with that proposed by Szichman and Baer, based on kinematic arguments, and found to be complementary, i.e., based on PES features. The excitation function shape shows a continuous increase with no saturation, owing to some high vibrational frequencies perpendicular to the reaction coordinate.

Comparison with experimental rate constants shows that calculated values are 1 order of magnitude lower than measured

ones. As a consequence, the PES must be improved in order to fit experimental data. However, this is a delicate task using QCT since error compensation may lead to incorrect corrections. More detailed information, from both experiment and theory, awaits for this refinement stage.

Acknowledgment. The authors thank financial support from the Spanish DGICYT (projects PB94−0909 and PB95-0598-W2-01), the Catalan CIRIT GRQ94-1008 grant, and the computer time generously allocated by the Centre de Computació i Comunicacions de Catalunya (C4). J.S. gratefully acknowledges a predoctoral fellowship from the Spanish DGICYT.

References and Notes

(1) *J. Chem. Soc., Faraday Trans.* **1997**, *93*: special issue on Quantum Theory of Chemical Reactions. Clary, D. C. *J. Phys. Chem.* **1994**, *98*, 10678. Bowman, J. M.; Schatz, G. C. *Annu. Rev. Phys. Chem.* **1995**, *46*, 169. Clary, D. C.; Echave, J. *Advances in Molecular Vibrations and Collision Dynamics*; Bowman, J. M., Ed.; JAI Press: Greenwich, CT, 1994; Vol. 2A, p 203. Zhang, D. H.; Zhang, J. Z. H. in *Dynamics of Molecules and Chemical Reactions;* Wyatt, R. E., Zhang, J. Z. H. Eds.; Marcel Dekker: New York, 1996; p 231. Zhang, J. Z. H.; Dai, J.; Wei, Z. *J. Phys. Chem.* **1997**, *101*, 2746.

(2) Kuppermann, A.; Hipes, P. G. *J. Chem. Phys.* **1986**, *84*, 5962. Haug, K.; D. W. Schwenke, D. W.; Shima, Y.; Truhlar, D. G.; Zhang, J. Z. H.; Kouri, D. J. *J. Phys. Chem.* **1986**, *90*, 6757. Linderberg, J. *Int. J. Quantum Chem. Quantum Chem. Symp.* **1986**, *19*, 467. Parker, G. A.; Pack, R. T.; Archer, B. J.; Walker, R. B. *Chem. Phys. Lett.* **1987**, *137*, 564. Zhang, J. Z. H.; Miller, W. H. *Chem. Phys. Lett.* **1988**, *153*, 465. Manolopoulos, D. E.; Wyatt, R. E. *Chem. Phys. Lett.* **1988**, *152*, 23. Schatz, G. C. *Chem. Phys. Lett.* **1988**, *150*, 92. Launay, J. M.; LeDourneuf, M. *Chem. Phys. Lett.* **1989**, *163*, 178. Neuhauser, D.; Baer, M. *J. Chem. Phys.* **1989**, *91*, 4651. Manolopoulos, D. E.; Clary, D. C. *Annu. Rep. Prog. Chem. C* **1989**, 95. Miller, W. H. *Annu. Rev. Phys. Chem.* **1990**, *41*, 245. Truhlar, D. G.; Schwenke, D. W.; Kouri, D. J. *J. Phys. Chem.* **1990**, *94*, 7346. Launay, J. M. In *Dynamical Processes in Molecular Physics;* Delgado-Barrio, G., Ed.; IOP: Bristol, U.K.; 1993.

(3) Bowman, J. M.; Wang, D. *Advances in Molecular Vibrations and Collision Dynamics*; Bowman, J. M., Ed.; JAI Press: Greenwich, CT, **1994**; Vol. 2B, p 187.

(4) Metz, R. B.; Thoemke, J. D.; Pfeiffer, J. M.; Crim, F. F. *J. Chem. Phys.* **1993**, *99*, 1744. Pfeifer, J. M.; Metz, R. B.; Thoemke, J. D.; Woods III, E.; Crim, F. F. *J. Chem. Phys.* **1996**, 104, 4490. Kreher, C.; Theinl, R; Gericke, K.-H. *J. Chem. Phys.* **1996**, 104, 4481.

(5) Zare, R. N. *Nature* **1993**, *365*, 105.

(6) Alagia, M.; Balucani, N.; Casavecchia, P.; Stranges, D.; Volpi, G. G. *J. Chem. Soc., Faraday Trans.* **1995**, *91*, 575.

(7) Metz, R. B.; Pfeiffer, J. M.; Thoemke, J. D.; Crim, F. F. *Chem. Phys. Lett.* **1994**, *221*, 347.

(8) Manolopoulos, D. E. *J. Chem. Phys.* **1986**, *85*, 6425.

(9) Manolopoulos, D. E.; Gray, S. K. *J. Chem. Phys.* **1995**, *102*, 9214

(10) Kuppermann, A. *Advances in Molecular Vibrations and Collision Dynamics*; Bowman, J. M., Ed.; JAI Press: Greenwich, CT, 1994; Vol. 2B, p 117.

(11) Colbert, D. T.; Miller, W. H. *J. Chem. Phys.* **1992**, *96*, 1982. Lill, J. V.; Parker, G. A.; Light, J. C. *Chem. Phys. Lett.* **1982**, *89*, 485. Echave, J.; Clary, D. C. *Chem. Phys. Lett.* **1992**, *190*, 225.

(12) Laganà, A. Ed. *Supercomputer algorithms for reactivity, dynamics and kinetics of small molecules*; Kluwer: Dordrecht, The Netherlands, 1989.

(13) Manthe, U.; Seideman, T.; Miller, W. H. *J. Chem. Phys.* **1993**, *99*, 10078.

(14) Neuhauser, D. *J. Chem. Phys.* **1994**, *100*, 9272.

(15) Zhang, D. H.; Zhang, J. Z. H. *J. Chem. Phys.* **1994**, *101*, 1146. Zhang, D. H.; Light, J. C. *J. Chem. Phys.* **1996**, *105*, 1291.

(16) Zewail, A. H. *Femtochemistry: Ultrafast Dynamics of the Chemical Bond*; World Scientific Series in 20th Century Chemistry; World Scientific Publishing Co. Pte. Ltd.: London, 1994; Vol. 3. Vítores, M.de C.; Candori, R.; Pirani, F.; Aquilanti, V.; Garay, M.; Ureña, A. G. *Chem. Phys. Lett.* **1996**, *263*, 456

(17) Page, M. *Comput. Phys. Commun.* **1994**, *84*, 115. Truhlar, D. G. in *The reaction Path in Chemistry: Current Approaches and Perspectives;* Heidrich, D., Ed.; Kluwer Academic: Dordrecht, The Netherlands, 1995; p 229. Peslherbe, G. H.; Hase, W. L. *J. Chem. Phys.* **1996**, *104*, 7882. Smith, B. R.; Bearpark, M. J.; Robb, M. A.; Bernardi, F.; Olivucci, M. *Chem. Phys. Lett.* **1995**, *242*, 27. Steckler, R.; Thurman, G. M.; Watts, J. D.; Bartlett, R. J. *J. Chem. Phys.* **1997**, *106*, 3926.

(18) Albertí, M.; Sayós, R.; Solé, A.; Aguilar, A. *J. Chem. Soc., Faraday Trans.* **1991**, *87*, 1057.

(19) Aguilar, A.; González, M.; Illas, F.; Rubio, J.; Sayós, R. *Chem. Phys.* **1992**, *161*, 99.

(20) Last, I.; Aguilar, A.; Gilibert, M.; Sayós, R. *J. Phys. Chem.* **1997**, *101*, 1206.

(21) Page, M. *J. Phys. Chem.* **1989**, *93*, 3639.

(22) Casavecchia, P. Unpublished data.

(23) Garland, N. L.; Stanton, C. T.; Nelson, H. H. *J. Chem. Phys.* **1991**, *95*, 2511.

(24) Murrell, J. N.; Carter, S.; Farantos, S. C.; Huxley. P.; Varandas, A. J. C. *Molecular Potential Energy Functions*; John Wiley & Sons: New York, 1984.

(25) Albertí. M.; Solé, A.; Aguilar, A.. *J. Chem. Soc., Faraday Trans.* **1991**, 87, 37.

(26) Albertí, M.; Prieto, M.; Aguilar, A. *J. Chem. Soc., Faraday Trans.* **1992**, *88*, 1615.

(27) Grande, X.; Albertí, M.; Giménez, X., Lucas, J. M.; Aguilar, A. *J. Chem. Soc., Faraday Trans.* **1993**, *89*, 1587.

(28) Albertí, M. Ph.D. Thesis, Departament de Química Física, Universitat de Barcelona, 1990.

(29) Sayós, R. Ph.D. Thesis, Departament de Química Física, Universitat de Barcelona, 1988.

(30) Schatz, G. C.; Elgersma, H. *Chem. Phys. Lett.* **1980**, *73*, 21.

(31) Sakai, S.; Jordan, K. D. *J. Phys. Chem.* **1983**, *87*, 2293.

(32) Sayós, R. POLQCT Program, Universitat de Barcelona, 1989 (unpublished).

(33) Porter, R. N.; Raff, L. M., *Dynamics of Molecular Collisions*; Miller, W. H. Ed.; Plenum Press: New York, 1976; Part B.

(34) Bradley, K. S.; Schatz, G. C. *J. Phys. Chem.* **1994**, *98*, 3788.

(35) Balakrishnan, N.; Billing, G. D. *J. Chem. Phys.* **1994**, *101*, 2785.

(36) Echave, J.; Clary, D. C. *J. Chem. Phys.* **1994**, *100*, 402.

(37) Szichman, H.; Last, I.; Baram, A.; Baer, M. *J. Phys. Chem.* **1993**, *97*, 6436.

(38) Szichman, H.; Baer, M. *J. Chem. Phys.* **1994**, *101*, 2081.

(39) Sun, Q.; Bowman, J. M. *J. Chem. Phys.* **1990**, *92*, 5201. Sun, Q.; Yang, D. L.; Wang, N. S.; Bowman, J. M. *J. Chem. Phys.* **1990**, *93*, 4730. Brooks, A. N.; Clary, D. C. *J. Chem. Phys.* **1990**, *92*, 4178.

(40) ter Horst, M. A.; Schatz, G. C.; Harding L. B. *J. Chem. Phys.* **1996**, *105*, 558.

(41) Takayanagi, T; Schatz, G. C. *J. Chem. Phys.* **1997**, *106*, 3227

(42) Laganà, A.; Aguilar, A.; Giménez, X.; Lucas, J. M. *Chem. Phys. Lett.* **1992**, *189*, 138.

(43) Giménez, X.; Lucas, J. M.; Aguilar, A.; Laganà, A. *J. Phys. Chem.* **1993**, *97*, 8578.

(44) Gilibert, M; Giménez, X.; González, M.; Sayós, R.; Aguilar, A. *Chem. Phys.* **1995**, *191*, 1.

(45) Aguilar, A.; Gilibert, M.; Giménez, X.; González, M.; Sayós, R. *J. Chem. Phys.* **1995**, *103*, 4496.

(46) Kudla, K.; Schatz, G. C. *Chem. Phys.* **1993**, *175*, 71.

(47) Szichman, H.; Baer, M. *J. Chem. Phys.* **1996**, *105*, 10380.